Research Square

Preprints are preliminary reports that have not undergone peer review.
They should not be considered conclusive, used to inform clinical practice,
or referenced by the media as validated information.

GCLC-dependent glutathione restrains NK cell-driven inflammation in tumor and autoimmune disease

Jie Yao

lyyaoj@scut.edu.cn

the Sixth Affiliated Hospital, School of Medicine, South China University of Technology (Nanhai District People's Hospital of Foshan)

Rongrong Song

the Sixth Affiliated Hospital, School of Medicine, South China University of Technology (Nanhai District People's Hospital of Foshan) https://orcid.org/0009-0003-7556-6500

Jieyu Zhang

the Sixth Affiliated Hospital, School of Medicine, South China University of Technology (Nanhai District People's Hospital of Foshan)

Yao Zeng

the Sixth Affiliated Hospital, School of Medicine, South China University of Technology (Nanhai District People's Hospital of Foshan)

Guozhi Yan

the Sixth Affiliated Hospital, School of Medicine, South China University of Technology (Nanhai District People's Hospital of Foshan)

Yanli Li

the Sixth Affiliated Hospital, School of Medicine, South China University of Technology (Nanhai District People's Hospital of Foshan)

Zhihao Li

the Sixth Affiliated Hospital, School of Medicine, South China University of Technology (Nanhai District People's Hospital of Foshan)

Article

Keywords: Natural killer cells, GCLC, glutathione, HIF-1a, tumor immunity, rheumatoid arthritis

Posted Date: November 20th, 2026

DOI: https://doi.org/10.21203/rs.3.rs-11452855/v1

License: This work is licensed under a Creative Commons Attribution 4.0 International License.
Read Full License

Additional Declarations: (Not answered)

GCLC-dependent glutathione restrains NK cell-driven inflammation in tumor and autoimmune disease

Running title: Glutathione and natural killer cell responses

Authors: Rongrong Song1, Jieyu Zhang1, Yao Zeng2, Guozhi Yan1, Yanli Li1, Zhihao Li1, Jie Yao1*

Affiliations: 1Department of Laboratory Medicine, School of Medicine, the Sixth Affiliated Hospital of South China University of Technology (Nanhai District People's Hospital of Foshan), Foshan, 528200, China.

2Shanxi University of Traditional Chinese Medicine, Yuci District, Jinzhong City, Shanxi Province, 030619, China.

Correspondence: Jie Yao lyyaoj@scut.edu.cn

Competing interests: The authors have declared that no conflict of interest exists.

Abstract

Glutathione (GSH) is a major intracellular redox buffer, but how GSH synthesis by glutamate-cysteine ligase catalytic subunit (GCLC) shapes natural killer (NK)-cell survival and effector function in tumor immunity and autoimmune inflammation remains unclear. Here, we investigated the consequences of Gclc deletion using NK-cell-specific and hematopoietic mouse models, tumor and autoimmune disease models, and human samples. Gclc deletion reduced NK-cell abundance, proliferation, survival, and terminal maturation across several tissues, but surviving NK cells showed enhanced acute effector responses. Mechanistically, GCLC dependent GSH regulates NK cell responses through the ROS-HIF-1α signaling pathway. NK cells in tumors and autoimmune diseases exhibit opposite levels of GCLC expression. High expression of GCLC in NK cells in tumors can inhibit their expression of HIF-1α and cytokines, thereby impairing their tumor control ability. NK cell GCLC expression decreases in RA and is associated with increased HIF-1α and effector factors. In summary, the synthesis of GSH dependent on GCLC shapes the effect of NK cells through the HIF-1 signaling pathway in a disease environment dependent manner, which is a key factor determining NK cell responses in tumor immune control and autoimmune inflammation.

Keyword: Natural killer cells; GCLC; glutathione; HIF-1α; tumor immunity; rheumatoid arthritis

1. Introduction

Natural killer (NK) cells are innate lymphocytes that recognize and eliminate infected or transformed cells without prior antigen sensitization[1–3]. NK-cell function is reflected in multiple readouts, including degranulation (CD107a), and the expression of cytotoxic molecules such as granzyme B[4–7]. In addition to direct cytotoxicity, they produce cytokines, including interferon-γ (IFN-γ), that shape broader immune responses[1,4,8,9]. These functions make NK cells important participants in tumor surveillance and autoimmune disease[1,2,10–12]. However, NK-cell activity depends on cellular fitness, maturation, and the tissue environment in which the cells operate[2,4,13,14].

Hypoxia-inducible factor 1 (HIF-1) is a context-dependent regulator of NK-cell responses[15–17]. Studies have reported that HIF-1α can influence NK-cell cytotoxicity and the production of effector molecules, including IFN-γ[16,18]. However, its reported effects differ with the activation state of NK cells and the experimental or tissue context[15,16,18,19]. HIF-1 may therefore help connect environmental conditions to NK-cell function, but the factors that determine whether HIF-1-associated responses support immune control or contribute to inflammation remain incompletely understood[15,20].

Glutathione (GSH) is a major intracellular redox buffer, and its synthesis depends on glutamate-cysteine ligase, whose catalytic subunit is encoded by GCLC[21,22]. By regulating cellular redox balance, GSH may influence reactive oxygen species (ROS)-associated signaling and, in turn, HIF-1α responses[23–27]. However, how GCLC-dependent GSH synthesis shapes HIF-1α expression and NK-cell effector readouts

remains unclear. In particular, it is not known whether GCLC loss affects NKp46^{+} NK cells and the broader CD3^{-}NK1.1^{+} NK-cell population in the same way, or how these population-specific responses relate to NK-cell survival and function in tumor and autoimmune inflammation settings[24,25,28,29].

We asked whether the contrasting NK-cell responses in tumor-associated immune suppression and autoimmune inflammatory stress are associated with differences in GCLC expression. We hypothesized that GCLC-dependent GSH availability restrains selected stress-associated effector responses while supporting NK-cell fitness. Using conditional Gclc deletion, hematopoietic GCLC insufficiency, bone-marrow chimeras, mouse disease models and human samples, we compared GCLC expression across disease settings and assessed NK-cell maintenance, maturation and function. We compared NKp46^{+} and CD3^{-}NK1.1^{+} readouts and tested GSH supplementation, HIF-1α inhibition and mitochondrial ROS scavenging to examine the contribution of ROS–HIF-1α-associated signaling.

2. Results

2.1. NK-cell GCLC expression differs across tumor and autoimmune disease settings

We first assessed whether NK-cell GCLC expression varied across disease settings. RNA-sequencing analysis showed higher GCLC expression in NK cells from B16 melanoma-bearing mice than in healthy controls (Figure 1A). In human peripheral blood, NK cells expressed more GCLC than the other major immune-cell populations

examined (Figure 1B). GCLC expression was also increased in NK cells from patients with non-small-cell lung cancer (NSCLC; Figure 1C).

The pattern differed in autoimmune disease. The frequency of NK cells was lower in patients with rheumatoid arthritis (RA) than in healthy controls (Figure 1D), and GCLC expression in RA NK cells was also reduced (Figure 1E). Similarly, the number of NK cells in patients with systemic lupus erythematosus (SLE) decreased (Figure 1F) and showed lower GCLC expression (Figure 1G). These findings revealed opposing patterns of NK-cell GCLC expression across tumor and autoimmune disease settings and prompted us to investigate the functional consequences of GCLC deficiency.

2.2. GCLC supports NK-cell maintenance, survival and terminal maturation

To determine the role of GCLC in NK cells, we examined mice with Ncr1-Cre-mediated Gclc deletion. Gclc deletion reduced NK-cell numbers in the spleen, bone marrow, liver, and lung, but not in the lymph nodes (Figure 2A). The reduction was more pronounced in the NKp46^{+} population (Figure 2B).

We next examined processes that could contribute to the reduced NK-cell abundance. Ki67 expression was decreased in splenic and bone-marrow NK cells following Gclc deletion (Figure 2C), whereas Annexin V staining was increased (Figure 2D), consistent with reduced proliferation and increased apoptosis. Eomes and T-bet expression also changed, with distinct patterns in the spleen and bone marrow (Supplementary Figure 1A, B). Analysis of CD27 and CD11b revealed fewer terminally mature CD11b^{+} CD27^{-} NK cells and a corresponding increase in less mature subsets in both compartments

(Figure 2E). The expression of CD117, CD127, and Ly49-family receptors was also altered (Supplementary Figure 1C,D). Together, these findings associate Gclc loss with impaired NK-cell maintenance and terminal maturation.

We then asked whether GCLC also contributes to earlier stages of NK-cell development. We therefore analyzed a Vav1-Cre model of hematopoietic GCLC insufficiency, because complete hematopoietic Gclc deficiency is incompatible with survival. Reduced GCLC expression was confirmed in this model (Supplementary Figure 1E). Hematopoietic GCLC insufficiency reduced the abundance of common lymphoid progenitors and NK progenitors, but did not substantially alter the abundance of hematopoietic stem cells, common myeloid progenitors, or pre-NK progenitors (Supplementary Figure 1F,G). As in the Ncr1-Cre model, CD27/CD11b analysis showed fewer terminally mature $CD11b^{+}CD27^{-}$ NK cells and an increase in less mature subsets (Figure 2F). Competitive bone-marrow chimeras further supported a cell-intrinsic contribution of GCLC: the proportion of terminally mature $CD11b^{+}CD27^{-}$ NK cells derived from GCLC-insufficient hematopoietic cells was reduced (Figure 2G). These findings indicate that GCLC contributes to NK-cell development, population maintenance, and terminal maturation.

2.3. GCLC deficiency is associated with altered HIF-1 signaling and mitochondrial abnormalities

To identify pathways associated with the Gclc-deficient phenotype, we performed RNA sequencing on control and Gclc-deficient NK cells. A total of 11 870 genes were

detected in both groups (Figure 3A). Of these, 1 072 were differentially expressed in Gclc-deficient NK cells, including 517 upregulated and 555 downregulated genes (Figure 3B). Gene set enrichment analysis identified enrichment of HIF-related signaling and mitophagy-associated pathways (Figure 3C, D); Figure 3E shows the expression patterns of genes related to HIF-1 signaling. Quantitative PCR showed increased expression of Hif1a, Hif1b, Hmox1, and Camk2b transcripts (Figure 3F), indicating altered expression of genes associated with HIF-1 signaling.

We next examined mitochondrial phenotypes. JC-1 analysis showed reduced mitochondrial membrane potential in NKp46^{+} cells following Ncr1-Cre-mediated Gclc deletion, with a similar reduction in the hematopoietic GCLC-insufficient model (Figure 3G). By contrast, mitochondrial membrane potential was unchanged when NK cells were defined as CD3^{-}NK1.1^{+} cells in the Ncr1-Cre model (Figure 3H). Thus, the observed change depended on the NK-cell population analyzed and was only detected in the NKp46-expressing population. MitoSOX fluorescence was increased in NKp46^{+} NK cells from Gclc-deficient mice (Figure 3I), consistent with increased mitochondrial oxidant-associated signal. MitoSOX fluorescence was also increased in NK1.1^{+} NK cells, although to a lesser extent than in NKp46^{+} NK cells (Figure 3J). Transmission electron microscopy further revealed disrupted mitochondrial cristae and mitochondrial autophagosomes in NK cells from Gclc$^{fl/fl}$ Ncr1-Cre and Gclc$^{fl/+}$ Vav1-Cre mice (Figure 3K), supporting the presence of mitochondrial abnormalities. Together, these findings link GCLC deficiency to mitochondrial abnormalities and altered HIF-1-related gene

expression.

2.4. GSH-sensitive ROS–HIF-1 signaling is associated with population-dependent acute NK-cell responses

Because Gclc loss impaired NK-cell maintenance, we first asked whether it also reduced acute effector function. In the NKp46^{+} population, surviving NK cells with Gclc deletion showed increased CD107a, IFN-γ, and granzyme B under basal conditions and following YAC-1 stimulation (Figure 4A–C). In contrast, the broader CD3^{-}NK1.1^{+} population showed reduced granzyme B and IFN-γ (Figure 4D,E). Acute killing of YAC-1 and β2-microglobulin-deficient target cells was also enhanced (Figure 4F, G). Thus, Gclc loss impaired NK-cell maintenance while enhancing acute effector responses in the surviving NK-cell population assessed in these assays.

We next tested whether the altered granzyme B responses were sensitive to GSH availability, HIF-1α inhibition, or mitochondrial ROS scavenging. In NKp46^{+} cells, GSH supplementation restored granzyme B levels in Gclc-deficient mice to control levels (Figure 4H), indicating that this response was reversible and sensitive to GSH availability. PX-478, an HIF-1α inhibitor, significantly reduced granzyme B but did not fully restore it to control levels (Figure 4I). Treatment with MitoTEMPO, a mitochondrial ROS scavenger, also restored granzyme B levels in Gclc-deficient NK cells to control levels (Figure 4J), supporting a contribution of mitochondrial ROS to the enhanced response in NKp46^{+} cells.

In CD3^{-}NK1.1^{+} cells, GSH, PX-478 and mito-TEMPO further reduced granzyme B

(Figure 4K–M). Both gates were assessed in parallel from the same samples under the same stimulation conditions. Thus, the direction of acute responses and their sensitivity to intervention depended on the population analyzed.

2.5. Gclc deletion reduces NK-cell abundance and function in tumor-bearing mice

The enhanced acute responses of surviving Gclc-deficient NK cells raised the question of whether these cells retained antitumor activity in vivo. In the B16 pulmonary metastasis model, Ncr1-Cre-mediated Gclc deletion increased lung tumor burden (Figure 5A). Tumor control was also impaired in the Lewis lung carcinoma (LLC) model (Figure 5B). Hematopoietic GCLC insufficiency produced a similar phenotype, increasing B16 metastatic burden and LLC tumor growth (Figure 5C, D). Thus, enhanced acute responses did not translate into preserved antitumor protection in these models.

Analysis of tumor-associated NK cells provided context for this finding. *Gclc*-deficient mice showed reduced NK-cell proportion in the tumor setting (Figure 5E). In addition, IFN-γ and TNF-α expression in tumor-associated NK cells was lower in Gclc-deficient mice than in wild-type tumor-bearing mice (Figure 5F, G). This differed from the enhanced acute responses observed in the assays described above, indicating that the phenotype observed in acute assays was not maintained in tumor-bearing animals.

In human samples, NK cells from patients with NSCLC showed increased GCLC expression and reduced IFN-γ production. GSH supplementation reduced HIF-1α production by NK cells from healthy donors to levels comparable to those observed in

NSCLC samples (Figure 5H). Meanwhile, GSH supplementation reduced the production of IFN - γ by healthy donor NK cells to levels comparable to those observed in NSCLC samples (Figure 5I). HIF-1α inhibition likewise reduced IFN-γ levels in healthy-donor NK cells to levels comparable to those in NSCLC samples (Figure 5J). These findings indicate that GCLC-associated NK-cell abundance and function are important for antitumor immunity in the models examined.

2.6. GSH and HIF-1α inhibition normalize excessive NK-cell responses in rheumatoid arthritis

We next examined this pathway in autoimmune inflammation. In the mouse model of rheumatoid arthritis, ankle-joint swelling was evident, with severe cases showing restricted joint movement (Figure 6A). Histological examination revealed synovial hyperplasia, extensive inflammatory-cell infiltration, and inflammatory exudates in the joint cavity. Proliferative synovial tissue extended into the joint cavity, forming granulation tissue with neovascularization and inflammatory-cell infiltration. Chondrocyte organization was disrupted, and focal cartilage erosion and surface defects were observed. These features were more severe following Gclc deletion (Figure 6B).

Splenic NK-cell proportion decreased in arthritic mice (Figure 6C). HIF-1α expression was increased in splenic NK cells during arthritis and was further elevated following Gclc deletion (Figure 6D). IFN-γ and Granzyme B levels were increased in NKp46^{+} NK cells from arthritic mice and further elevated following Gclc deletion (Figure 6E,F). In CD3^{-}NK1.1^{+}NK cells of arthritis mice, Granzyme B levels were elevated but did not

differ after Gclc deletion (Supplementary Figure 1H). These results suggest that the worsening of rheumatoid arthritis caused by GCLC deficiency may be solely due to the NKp46^{+} NK cell population.

In Gclc-deficient arthritic mice, GSH supplementation restored granzyme B levels to those of controls (Figure 6G). HIF-1α inhibition also restored granzyme B levels to control levels (Figure 6H). Thus, both GSH supplementation and HIF-1α inhibition normalized this NK-cell effector readout. A similar pattern was observed in human RA samples. NK cells from patients with RA showed increased HIF-1α expression, which decreased following GSH supplementation (Figure 6I). Granzyme B levels were also elevated relative to those in healthy-donor NK cells and returned to control levels following GSH supplementation (Figure 6J).

3. Discussion

GCLC-dependent GSH synthesis links NK-cell fitness to context-dependent effector responses. *Gclc* deletion impaired maintenance and maturation, while acute responses increased in NKp46^{+} cells but decreased in the broader CD3^{-}NK1.1^{+} gate. These findings distinguish population maintenance from selected acute functional readouts.

The reduction in NK-cell abundance and terminal maturation extends evidence that NK-cell development and homeostasis depend on coordinated cytokine signaling and cellular fitness[30,31]. NK cells undergo defined maturation stages associated with changes in proliferative capacity and function[32,32–35]. IL-15–mTOR signaling supports NK-cell development, expansion, and effector potential [36–41], while disruption of these

pathways can impair NK-cell number, maturation, and function [36,40]. Our findings add GCLC-dependent GSH synthesis to this framework: Gclc deletion was associated with reduced proliferation, increased apoptosis, impaired terminal maturation, and altered progenitor abundance. The competitive bone-marrow chimera results further support a cell-intrinsic contribution of GCLC to NK-cell maturation.

The opposing acute readouts arose from the same samples under identical stimulation, but the gates are not mutually exclusive[42,43]. The broader $CD3^{-}NK1.1^{+}$ gate includes NK cells at different maturation stages and may integrate responses from cells with different phenotypes and functional states[32,44]. $NKp46^{+}$ analysis aligns more closely with Ncr1-Cre targeting, although other NKp46-expressing innate lymphoid populations may also be affected[45,46]. Previous mouse and human studies linked GCLC loss to impaired viability or function[2425]. Our results qualify those findings by showing that a decrease in the broad-gate readout can coexist with increased acute responses in the $NKp46^{+}$ gate.

The mitochondrial and HIF-1α-associated findings provide a potential framework for understanding these population-dependent effects. Gclc-deficient NK cells showed mitochondrial abnormalities and increased MitoSOX fluorescence, while transcriptomic and quantitative PCR analyses indicated altered HIF-1-associated signals. GSH supplementation, HIF-1α inhibition, and mitochondrial ROS scavenging modified selected effector readouts. Together, these observations support an association between GCLC-dependent redox control and HIF-1α-associated NK-cell responses. They do not establish a single causal sequence from GCLC loss through mitochondrial

ROS and HIF-1α to effector activity. MitoSOX and mitochondrial membrane-potential measurements are indirect indicators of mitochondrial state, and pharmacological interventions can have effects beyond their intended targets[23,47–50].

The effects of HIF-1α on NK cells vary with cell state and experimental setting[19,51]. HIF-1α deletion has been reported to enhance activation-associated features of tumor-infiltrating NK cells and reduce tumor growth in one model[17]. In another, HIF-1α deletion altered tumor growth through effects on NK-cell recruitment and angiogenesis, despite reduced tumor-cell killing[16]. Conversely, HIF-1α can support resting NK-cell homeostasis and selected responses of activated NK cells under hypoxia[15,18,19,52]. Hypoxia can also alter activating-receptor expression and NK-cell effector function [51,53]. These findings suggest that the HIF-1α-associated responses observed after Gclc deletion may differ between acute assays and diseased tissues. Our results show that HIF-1α inhibition modified granzyme B readouts, but do not determine whether HIF-1α directly causes the divergence between NKp46^{+} and CD3^{-}NK1.1^{+} populations.

The opposing patterns of GCLC expression across tumor and autoimmune settings support our central hypothesis that GCLC-dependent redox regulation is associated with contrasting NK-cell functional states. NK cells from tumor-bearing mice and patients with NSCLC showed increased GCLC expression, whereas RA NK cells showed reduced expression. Low GCLC expression in RA was accompanied by enhanced granzyme B responses, paralleling the heightened acute responses of surviving Gclc-deficient NKp46^{+} cells. GSH supplementation reduced granzyme B in

both settings, supporting the GSH sensitivity of this effector activation. In healthy-donor NK cells, GSH also reduced HIF-1α and IFN-γ to levels comparable to those in NSCLC samples. Together, these findings suggest that GCLC-dependent GSH availability may help restrain selected NK-cell effector responses and contribute to the functional differences between tumor-associated immune suppression and autoimmune inflammatory stress.

Enhanced acute NKp46^{+} responses did not preserve tumor protection, consistent with the importance of NK-cell abundance, persistence and local function[24,54–57]. The human expression and ex vivo treatment data support the proposed association, but do not establish that increased GCLC in NSCLC causes reduced HIF-1α or IFN-γ.

The arthritis findings support GSH-sensitive modulation of selected NK-cell responses. However, the interventions measured NK-cell readouts and did not establish reversal of joint pathology. Previous studies implicate NK cells or their granulocyte–macrophage colony-stimulating factor in joint inflammation[58–60], whereas others report reduced peripheral activity or compartment-dependent changes[61–67]. Our findings therefore do not establish that the NKp46^{+} population alone drives arthritis exacerbation.

Further limitations concern population definition and targeting. The cellular basis of the opposing gates remains unresolved, and hematopoietic models do not establish NK-cell specificity for every in vivo phenotype68. Human ex vivo findings also do not demonstrate clinical efficacy or safety of GSH or HIF-1α-directed interventions.

Together, GCLC-dependent GSH synthesis supports NK-cell fitness while shaping

effector responses according to population and disease context. Future studies resolving NKp46^{+} and NKp46^{-} subsets, responder frequency and per-cell intensity, alongside cell-specific pathway perturbation, should clarify the cellular basis and causal order of ROS–HIF-1α-associated regulation.

4. Materials and methods

4.1. Human participants and sample processing

Peripheral blood samples were obtained from healthy donors and patients with non-small-cell lung cancer, rheumatoid arthritis and systemic lupus erythematosus. Human studies were approved by the local ethical committee. Informed consent was obtained from all participants.

4.2. Mouse models

Gclc-floxed mice (CKOCMP-14629-*Gclc*-B6J-VA, Cyanen) were crossed with Vav1-Cre mice (BL6/Vav1 cre; C001019, Cyanen) or Ncr1-Cre mice [BL6/JGpt-Ncr1em1cin (iCre P2A)/Gpt; T005674, GemPharmatech]. Complete hematopoietic *Gclc* deficiency was incompatible with survival; $Gclc^{fl/+}$ Vav1-Cre and $Gclc^{fl/fl}$ Ncr1-Cre mice were therefore studied. Experiments used 10-week-old male or female mice. Protocols were approved by the Animal Ethics Committee of the Sixth Affiliated Hospital of South China University of Technology.

4.3. Antibodies and flow cytometry

Single-cell suspensions were prepared from peripheral blood, spleen, bone marrow,

liver, lung, lymph nodes and tumor-bearing tissues. Murine NK cells were identified using NKp46^{+} or CD3^{-}NK1.1^{+} gates, as indicated.

NK-cell maturation, proliferation and apoptosis were assessed using CD27/CD11b, Ki67 and Annexin V, respectively. Effector measurements included CD107a, IFN-γ, granzyme B and tumor necrosis factor-α. Additional markers included Eomes, T-bet, CD117, CD127, Ly49-family receptors, CD98, CD71, GCLC and HIF-1α. Antibodies were purchased from Invitrogen and Abcam. Surface staining used antibodies in 100 µl phosphate-buffered saline containing 2% fetal bovine serum, followed by washing and flow cytometry. For intracellular staining, cells were fixed, permeabilized, stained with specific antibodies, washed and analyzed by flow cytometry.

4.4. NK-cell stimulation and cytotoxicity assays

Mice received intraperitoneal polyinosinic:polycytidylic acid (200 µg per mouse) 18 h before spleen collection. Splenocytes were cultured in complete RPMI-1640 alone, with YAC-1 cells (2×10^{6} cells), or with the positive-control stimulant P+I for 1 h. Golgi and endoplasmic reticulum inhibitors and anti-CD107a were then added for a further 4 h. Cells underwent surface and intracellular staining for IFN-γ and granzyme B before flow cytometry.

For β2-microglobulin-deficient target clearance, wild-type and β2m−/− splenocytes were labeled with Violet-450 and carboxyfluorescein succinimidyl ester, respectively. Equal numbers were mixed and injected intravenously into pretreated mice. Their ratio in the spleen and lymph nodes was measured after 6 h.

For YAC-1 clearance, wild-type splenocytes and YAC-1 cells were labeled with carboxyfluorescein succinimidyl ester and Violet, respectively, mixed and injected intraperitoneally into pretreated mice. Their ratio in peritoneal lavage fluid was measured after 6 h to calculate rejection.

4.5. RNA sequencing and computational analysis

Splenic NK cells from control and *Gclc*-deficient mice were sorted using a BD flow cytometer. RNA was extracted and assessed using an Agilent 2100 Bioanalyzer. Libraries were prepared using NEB standard or strand-specific protocols. Reads were aligned to the reference genome using HISAT2. Differentially expressed genes underwent Gene Ontology and Kyoto Encyclopedia of Genes and Genomes enrichment analysis using clusterProfiler.

4.6. Quantitative PCR

NK-cell RNA was reverse-transcribed using HiScript II Q RT SuperMix for qPCR (Vazyme). Quantitative PCR used ChamQ SYBR qPCR Master Mix (Vazyme). Primer sequences (5′–3′; forward/reverse) were:

HIF-1α: CCTGCACTGAATCAAGAGGTTGC / CCATCAGAAGGACTTGCTGGCT;
HIF-1β: CTGGGTCCCACCATTGCTTC / CGTCGCTTAATAGCCCTCTGT;
Camk2b: AAGCAGGCGGAAGACATTAGG / AGTTTCTGAGTCCTCTTGTCCT;
Hmox1: CACTCTGGAGATGACACCTGAG / GTGTTCCTCTGTCAGCATCACC;
β-actin: CATTGCTGACAGGATGCAGAAGG /

TGCTGGAAGGTGGACAGTGAGG.

4.7. MitoSOX and mitochondrial membrane potential

JC-1 (Thermo Fisher Scientific; 1 mg/ml stock in dimethyl sulfoxide) was diluted to 2.5 μg/ml in RPMI-1640. Cells were stained at 37 °C for 30 min in the dark. Staining was stopped with 4% fetal bovine serum in phosphate-buffered saline. Cells were washed, resuspended in 2% fetal bovine serum in phosphate-buffered saline and analyzed for phycoerythrin and fluorescein isothiocyanate fluorescence.

MitoSOX Red (Thermo Fisher Scientific; 5 mM stock in dimethyl sulfoxide) was diluted to 500 nM in RPMI-1640. Staining and washing followed the same conditions as for JC-1. Phycoerythrin fluorescence was measured using a Beckman Coulter flow cytometer.

4.8. Transmission electron microscopy

Splenic NK cells were purified using a CD49b selection kit, centrifuged and fixed in electron microscopy fixative at 4 °C for ≥30 min. Sections were examined by transmission electron microscopy for mitochondrial and endoplasmic reticulum morphology, size and abundance, and for autophagosomes. Perinuclear mitochondria were imaged using the nucleus as a reference.

4.9. Competitive bone-marrow chimeras and progenitor analysis

CD45.1/CD45.2 recipients received 8 Gy irradiation, followed by tail-vein injection of wild-type CD45.1 and *Gclc*$^{fl/+}$ Vav1-Cre CD45.2 bone-marrow cells (2.5×10^6 each).

After 8 weeks, splenocytes were analyzed for CD45.1, CD45.2, CD3, NK1.1, CD11b and CD27 by flow cytometry.

4.10. Tumor models

LLC or B16 cells (5×10^6 per mouse) were injected intravenously. Cells were cultured in Dulbecco's modified Eagle medium with 10% fetal bovine serum and 1% penicillin/streptomycin, and detached with 0.25% trypsin at 70% confluence. After 21–28 days, lungs were photographed, nodules counted and single-cell suspensions prepared for NK-cell analysis.

4.11. Experimental arthritis

Chicken type II collagen (10 mg/ml) was dissolved in 0.05 M acetic acid overnight at 4 °C and emulsified 1:1 with complete adjuvant. Control and NK-cell-targeted Gclc-deficient mice received 200 μl subcutaneously at the tail base and legs. Collagen in incomplete adjuvant was administered on day 21, followed by intraperitoneal lipopolysaccharide (50 μg) on day 28. On day 30, joint swelling was evaluated, knee and ankle sections underwent hematoxylin and eosin staining, and splenic NK-cell HIF-1α and effector responses were assessed.

4.12. Mitochondrial ROS scavenging, GSH supplementation and HIF-1α inhibition

Cells were treated with mito-TEMPO (Aladdin, M414479; 5 μM) for 48 h, GSH (Aladdin, G121372; 2 mM) for 48–72 h, or PX-478 (Targeted Mol; 40 μM) for 48 h.

Control groups were included. Granzyme B was measured after mito-TEMPO treatment; HIF-1α, IFN-γ and granzyme B after GSH; and IFN-γ and granzyme B after PX-478.

4.13. Statistical analysis

Statistical analyses were performed using GraphPad Prism 10.0 (GraphPad Software, San Diego, USA). Data are presented as mean ± standard error of the mean (SEM). Comparisons between two independent groups were analysed using unpaired Student's t tests. Comparisons between matched control and treated samples in the GSH rescue, PX-478 treatment and mito-TEMPO treatment experiments were analysed using paired Student's t tests. Two-way analysis of variance was used where appropriate. $P < 0.05$ was considered statistically significant.

References

1 Vivier E, Raulet DH, Moretta A, Caligiuri MA, Zitvogel L, Lanier LL *et al.* Innate or Adaptive Immunity? The Example of Natural Killer Cells. *Science* 2011; **331**: 44–49.

2 Morvan MG, Lanier LL. NK cells and cancer: you can teach innate cells new tricks. *Nat Rev Cancer* 2016; **16**: 7–19.

3 Laskowski TJ, Biederstädt A, Rezvani K. Natural killer cells in antitumour adoptive cell immunotherapy. *Nat Rev Cancer* 2022; **22**: 557–575.

4 Chen S, Zhu H, Jounaidi Y. Comprehensive snapshots of natural killer cells functions, signaling, molecular mechanisms and clinical utilization. *Signal Transduct Target Ther* 2024; **9**: 302.

5 Prager I, Liesche C, van Ooijen H, Urlaub D, Verron Q, Sandström N *et al.* NK cells switch from granzyme B to death receptor-mediated cytotoxicity during serial

killing. *J Exp Med* 2019; **216**: 2113–2127.

6 Smyth MJ, Hayakawa Y, Takeda K, Yagita H. New aspects of natural-killer-cell surveillance and therapy of cancer. *Nat Rev Cancer* 2002; **2**: 850–861.

7 Alter G, Malenfant JM, Altfeld M. CD107a as a functional marker for the identification of natural killer cell activity. *Journal of Immunological Methods* 2004; **294**: 15–22.

8 Bryceson YT, Fauriat C, Nunes JM, Wood SM, Björkström NK, Long EO *et al.* Functional Analysis of Human NK Cells by Flow Cytometry. In: Campbell KS (ed). *Natural Killer Cell Protocols: Cellular and Molecular Methods*. Humana Press: Totowa, NJ, 2010, pp 335–352.

9 Moretta A, Marcenaro E, Parolini S, Ferlazzo G, Moretta L. NK cells at the interface between innate and adaptive immunity. *Cell Death Differ* 2008; **15**: 226–233.

10 Vivier E, Ugolini S, Blaise D, Chabannon C, Brossay L. Targeting natural killer cells and natural killer T cells in cancer. *Nat Rev Immunol* 2012; **12**: 239–252.

11 Wolf NK, Kissiov DU, Raulet DH. Roles of natural killer cells in immunity to cancer, and applications to immunotherapy. *Nat Rev Immunol* 2023; **23**: 90–105.

12 Yang Y, Day J, Souza-Fonseca Guimaraes F, Wicks IP, Louis C. Natural killer cells in inflammatory autoimmune diseases. *Clin & Trans Imm* 2021; **10**: e1250.

13 Sun JC, Lanier LL. NK cell development, homeostasis and function: parallels with $CD8^+$ T cells. *Nat Rev Immunol* 2011; **11**: 645–657.

14 Dogra P, Rancan C, Ma W, Toth M, Senda T, Carpenter DJ *et al.* Tissue Determinants of Human NK Cell Development, Function, and Residence. *Cell* 2020; **180**: 749-763.e13.

15 Pelletier A, Nelius E, Fan Z, Khatchatourova E, Alvarado-Diaz A, He J *et al.* Resting natural killer cell homeostasis relies on tryptophan/NAD+ metabolism and HIF-1α. *EMBO Rep* 2023; **24**: e56156.

16 Krzywinska E, Kantari-Mimoun C, Kerdiles Y, Sobecki M, Isagawa T, Gotthardt D *et al.* Loss of HIF-1α in natural killer cells inhibits tumour growth by stimulating non-productive angiogenesis. *Nat Commun* 2017; **8**: 1597.

17 Ni J, Wang X, Stojanovic A, Zhang Q, Wincher M, Bühler L *et al.* Single-Cell RNA Sequencing of Tumor-Infiltrating NK Cells Reveals that Inhibition of Transcription Factor HIF-1α Unleashes NK Cell Activity. *Immunity* 2020; **52**: 1075-1087.e8.

18 Cluff E, Magdaleno CC, Fernandez E, House T, Swaminathan S, Varadaraj A *et al.*

Hypoxia-inducible factor-1 alpha expression is induced by IL-2 via the PI3K/mTOR pathway in hypoxic NK cells and supports effector functions in NKL cells and ex vivo expanded NK cells. *Cancer Immunol Immunother* 2022; **71**: 1989–2005.

19 Lim SA, Moon Y, Shin MH, Kim T-J, Chae S, Yee C *et al.* Hypoxia-Driven HIF-1α Activation Reprograms Pre-Activated NK Cells towards Highly Potent Effector Phenotypes via ERK/STAT3 Pathways. *Cancers (Basel)* 2021; **13**: 1904.

20 Giorgetta S, Cortopassi F, Chanis T, Ni J, Correia MP, Sticht C *et al.* Functional segregation of HIF-1α and AhR controls NK cell responsiveness under hypoxia. *iScience* 2026; **29**: 115492.

21 Lu SC. Glutathione synthesis. *Biochim Biophys Acta* 2013; **1830**: 3143–3153.

22 Lu SC. Regulation of glutathione synthesis. *Molecular Aspects of Medicine* 2009; **30**: 42–59.

23 Forman HJ, Zhang H, Rinna A. Glutathione: overview of its protective roles, measurement, and biosynthesis. *Mol Aspects Med* 2009; **30**: 1–12.

24 Guerra L, Grusdat M, Kobayashi T, Longworth J, Kurniawan H, Franchina DG *et al.* Glutathione is critical for NK cell-mediated immunity. *Cell Rep* 2026; **45**: 116986.

25 Li JH, Feng Q, Ball AB, Lee CD, Wallerius ML, Bormin JG *et al.* Species-specific serine metabolism differentially controls natural killer cell functions. *Nat Metab* 2025; **7**: 1905–1923.

26 Zhang H, Forman HJ. Glutathione synthesis and its role in redox signaling. *Seminars in Cell & Developmental Biology* 2012; **23**: 722–728.

27 Hagen T. Oxygen versus Reactive Oxygen in the Regulation of HIF-1 α : The Balance Tips. *Biochemistry Research International* 2012; **2012**: 1–5.

28 Liu M, Liang S, Zhang C. NK Cells in Autoimmune Diseases: Protective or Pathogenic? *Front Immunol* 2021; **12**: 624687.

29 Schleinitz N, Vély F, Harlé J, Vivier E. Natural killer cells in human autoimmune diseases. *Immunology* 2010; **131**: 451–458.

30 Townsend MJ, Weinmann AS, Matsuda JL, Salomon R, Farnham PJ, Biron CA *et al.* T-bet regulates the terminal maturation and homeostasis of NK and Valpha14i NKT cells. *Immunity* 2004; **20**: 477–494.

31 Kennedy MK, Glaccum M, Brown SN, Butz EA, Viney JL, Embers M *et al.* Reversible Defects in Natural Killer and Memory Cd8 T Cell Lineages in Interleukin 15–Deficient Mice. *J Exp Med* 2000; **191**: 771–780.

32 Chiossone L, Chaix J, Fuseri N, Roth C, Vivier E, Walzer T. Maturation of mouse NK cells is a 4-stage developmental program. *Blood* 2009; **113**: 5488–5496.

33 Pfefferle A, Jacobs B, Haroun-Izquierdo A, Kveberg L, Sohlberg E, Malmberg K-J. Deciphering Natural Killer Cell Homeostasis. *Front Immunol* 2020; **11**: 812.

34 Gordon SM, Chaix J, Rupp LJ, Wu J, Madera S, Sun JC *et al.* The transcription factors T-bet and Eomes control key checkpoints of natural killer cell maturation. *Immunity* 2012; **36**: 55–67.

35 Caligiuri MA. Human natural killer cells. *Blood* 2008; **112**: 461–469.

36 Yang M. NK cell development requires Tsc1-dependent negative regulation of IL-15-triggered mTORC1 activation. *NATURE COMMUNICATIONS*.

37 Ali AK, Nandagopal N, Lee S-H. IL-15-PI3K-AKT-mTOR: A Critical Pathway in the Life Journey of Natural Killer Cells. *Front Immunol* 2015; **6**: 355.

38 Yang C, Malarkannan S. Transcriptional Regulation of NK Cell Development by mTOR Complexes. *Front Cell Dev Biol* 2020; **8**. doi:10.3389/fcell.2020.566090.

39 Marçais A, Cherfils-Vicini J, Viant C, Degouve S, Viel S, Fenis A *et al.* The metabolic checkpoint kinase mTOR is essential for IL-15 signaling during the development and activation of NK cells. *Nat Immunol* 2014; **15**: 749–757.

40 Donnelly RP, Loftus RM, Keating SE, Liou KT, Biron CA, Gardiner CM *et al.* mTORC1-dependent metabolic reprogramming is a prerequisite for Natural Killer cell effector function. *J Immunol* 2014; **193**: 4477–4484.

41 Keppel MP, Topcagic N, Mah AY, Vogel TP, Cooper MA. Activation-specific metabolic requirements for NK cell IFN-γ production. *J Immunol* 2015; **194**: 1954–1962.

42 Klose CSN, Flach M, Möhle L, Rogell L, Hoyler T, Ebert K *et al.* Differentiation of type 1 ILCs from a common progenitor to all helper-like innate lymphoid cell lineages. *Cell* 2014; **157**: 340–356.

43 Satoh-Takayama N, Vosshenrich CAJ, Lesjean-Pottier S, Sawa S, Lochner M, Rattis F *et al.* Microbial flora drives interleukin 22 production in intestinal NKp46+ cells that provide innate mucosal immune defense. *Immunity* 2008; **29**: 958–970.

44 Zhang J, Le Gras S, Pouxvielh K, Faure F, Fallone L, Kern N *et al.* Sequential actions of EOMES and T-BET promote stepwise maturation of natural killer cells. *Nat Commun* 2021; **12**: 5446.

45 Vonarbourg C, Mortha A, Bui VL, Hernandez P, Kiss EA, Hoyler T *et al.* Progressive

loss of RORγt expression confers distinct functional fates to natural killer cell receptor-expressing RORγt+ innate lymphocytes. *Immunity* 2010; **33**: 736–751.

46 Satoh-Takayama N, Dumoutier L, Lesjean-Pottier S, Ribeiro VSG, Mandelboim O, Renauld J-C *et al.* The natural cytotoxicity receptor NKp46 is dispensable for IL-22-mediated innate intestinal immune defense against Citrobacter rodentium. *J Immunol* 2009; **183**: 6579–6587.

47 Dikalov SI, Harrison DG. Methods for Detection of Mitochondrial and Cellular Reactive Oxygen Species. *Antioxid Redox Signal* 2014; **20**: 372–382.

48 Perry SW, Norman JP, Barbieri J, Brown EB, Gelbard HA. Mitochondrial membrane potential probes and the proton gradient: a practical usage guide. *Biotechniques* 2011; **50**: 98–115.

49 Bain J, Plater L, Elliott M, Shpiro N, Hastie CJ, Mclauchlan H *et al.* The selectivity of protein kinase inhibitors: a further update. *Biochem J* 2007; **408**: 297–315.

50 Guerra C, Johal K, Morris D, Moreno S, Alvarado O, Gray D *et al.* Control of Mycobacterium tuberculosis growth by activated natural killer cells. *Clin Exp Immunol* 2012; **168**: 142–152.

51 Balsamo M, Manzini C, Pietra G, Raggi F, Blengio F, Mingari MC *et al.* Hypoxia downregulates the expression of activating receptors involved in NK-cell-mediated target cell killing without affecting ADCC. *Eur J Immunol* 2013; **43**: 2756–2764.

52 Velásquez SY, Killian D, Schulte J, Sticht C, Thiel M, Lindner HA. Short Term Hypoxia Synergizes with Interleukin 15 Priming in Driving Glycolytic Gene Transcription and Supports Human Natural Killer Cell Activities. *J Biol Chem* 2016; **291**: 12960–12977.

53 Sarkar S, Germeraad WTV, Rouschop KMA, Steeghs EMP, van Gelder M, Bos GMJ *et al.* Hypoxia Induced Impairment of NK Cell Cytotoxicity against Multiple Myeloma Can Be Overcome by IL-2 Activation of the NK Cells. *PLoS One* 2013; **8**: e64835.

54 Tumino N, Nava Lauson CB, Tiberti S, Besi F, Martini S, Fiore PF *et al.* The tumor microenvironment drives NK cell metabolic dysfunction leading to impaired antitumor activity. *International Journal of Cancer* 2023; **152**: 1698–1706.

55 Stojanovic A, Correia MP, Cerwenka A. Shaping of NK Cell Responses by the Tumor Microenvironment. *Cancer Microenvironment* 2013; **6**: 135–146.

56 Domagala J, Lachota M, Klopotowska M, Graczyk-Jarzynka A, Domagala A, Zhylko A *et al.* The Tumor Microenvironment—A Metabolic Obstacle to NK Cells' Activity. *Cancers (Basel)* 2020; **12**: 3542.

57 Michelet X, Dyck L, Hogan A, Loftus RM, Duquette D, Wei K *et al.* Metabolic

reprogramming of natural killer cells in obesity limits antitumor responses. *Nature Immunology* 2018; **19**: 1330–1340.

58 Wu L, Wang R, Zhou Y, Zhao D, Chen F, Wu X *et al.* Natural Killer Cells Infiltration in the Joints Exacerbates Collagen-Induced Arthritis. *Front Immunol* 2022; **13**. doi:10.3389/fimmu.2022.860761.

59 Louis C, Fonseca-Guimaraes FS-, Yang Y, D'Silva D, Kratina T, Dagley L *et al.* NK cell–derived GM-CSF potentiates inflammatory arthritis and is negatively regulated by CIS. *J Exp Med* 2020; **217**: e20191421.

60 Söderström K, Stein E, Colmenero P, Purath U, Müller-Ladner U, de Matos CT *et al.* Natural killer cells trigger osteoclastogenesis and bone destruction in arthritis. *Proc Natl Acad Sci U S A* 2010; **107**: 13028–13033.

61 Shegarfi H, Naddafi F, Mirshafiey A. Natural Killer Cells and Their Role in Rheumatoid Arthritis: Friend or Foe? *The Scientific World Journal* 2012; **2012**: 491974.

62 Aramaki T, Ida H, Izumi Y, Fujikawa K, Huang M, Arima K *et al.* A significantly impaired natural killer cell activity due to a low activity on a per-cell basis in rheumatoid arthritis. *Mod Rheumatol* 2009; **19**: 245–252.

63 Tak PP, Kummer JA, Hack CE, Daha MR, Smeets TJM, Erkelens GW *et al.* Granzyme-positive cytotoxic cells are specifically increased in early rheumatoid synovial tissue. *Arthritis & Rheumatism* 1994; **37**: 1735–1743.

64 Dobloug JH, Førre O, Kvien TK, Egeland T, Degré M. Natural killer (NK) cell activity of peripheral blood, synovial fluid, and synovial tissue lymphocytes from patients with rheumatoid arthritis and juvenile rheumatoid arthritis. *Annals of the Rheumatic Diseases* 1982; **41**: 490–494.

65 Combe B, Pope R, Darnell B, Talal N. Modulation of natural killer cell activity in the rheumatoid joint and peripheral blood. *Scand J Immunol* 1984; **20**: 551–558.

66 Yamin R, Berhani O, Peleg H, Aamar S, Stein N, Gamliel M *et al.* High percentages and activity of synovial fluid NK cells present in patients with advanced stage active Rheumatoid Arthritis. *Sci Rep* 2019; **9**: 1351.

67 Qiao J, Zhou M, Li Z, Ren J, Gao G, Zhen J *et al.* Elevated serum granzyme B levels are associated with disease activity and joint damage in patients with rheumatoid arthritis. *J Int Med Res* 2020; **48**: 0300060520962954.

Author Contributions

Rongrong Song: formal analysis, investigation; Jieyu Zhang: writing–original draft, data curation; Yao Zeng: data curation, investigation, Zhihao Li: data curation, Yanli Li: methodology; Guozhi Yan: Visualization; Jie,Yao: conceptualization, funding acquisition, writing – review and editing.

Ethics Statement

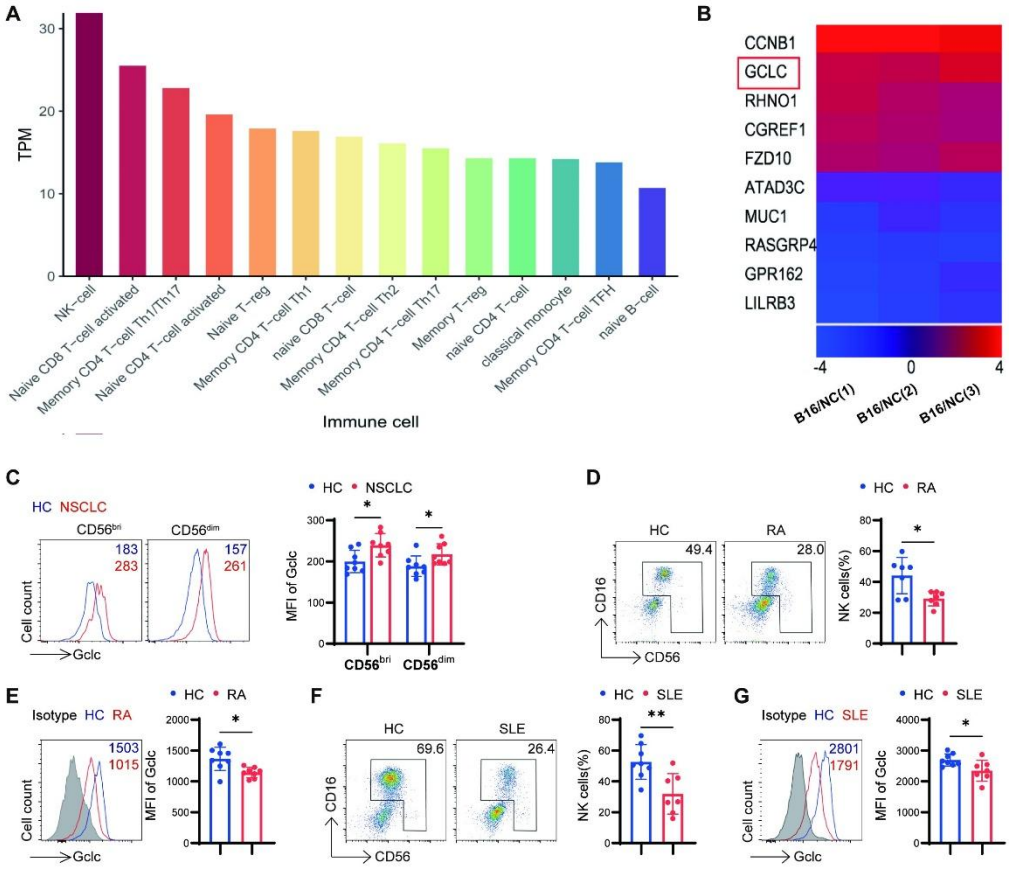
Human studies were approved by the Medical Ethics Committee of Nanhai District People's Hospital in Foshan City. Informed consent was obtained from all participants. Animal protocols were approved by the Animal Ethics Committee of the Sixth Affiliated Hospital of South China University of Technology.

Funding

This work was supported by the Guangdong Yiyang Healthcare Charity Foundation (grant no. JZ2024089; principal investigator: Jie Yao).

Availability of Data and Materials

Correspondence and requests for materials should be addressed to Jie Yao.



592

593

594 **Figure 1. NK-cell GCLC expression differs across tumor and autoimmune disease**

595 **settings.**

A GCLC expression in NK cells from healthy control mice and B16 melanoma-bearing mice, assessed by RNA sequencing. **B** GCLC expression in NK cells and other major immune-cell populations in human peripheral blood. **C** GCLC mean fluorescence intensities (MFI) in $CD56^{bright}$ and $CD56^{dim}$ NK cells from patients with non-small-cell lung cancer (NSCLC) and healthy controls. **D, E** Frequency of NK cells and GCLC MFI in total NK cells, respectively, in patients with rheumatoid arthritis (RA) and healthy controls (HC). **F, G** The number of NK cells (F) and the mean fluorescence intensities of GCLC (G) in patients with systemic lupus erythematosus (SLE) and healthy controls. Data are representative of, at least, 7 independent experiments and presented as means ± SEM. *P < 0.05, **P < 0.01 (n = 7 to 8).

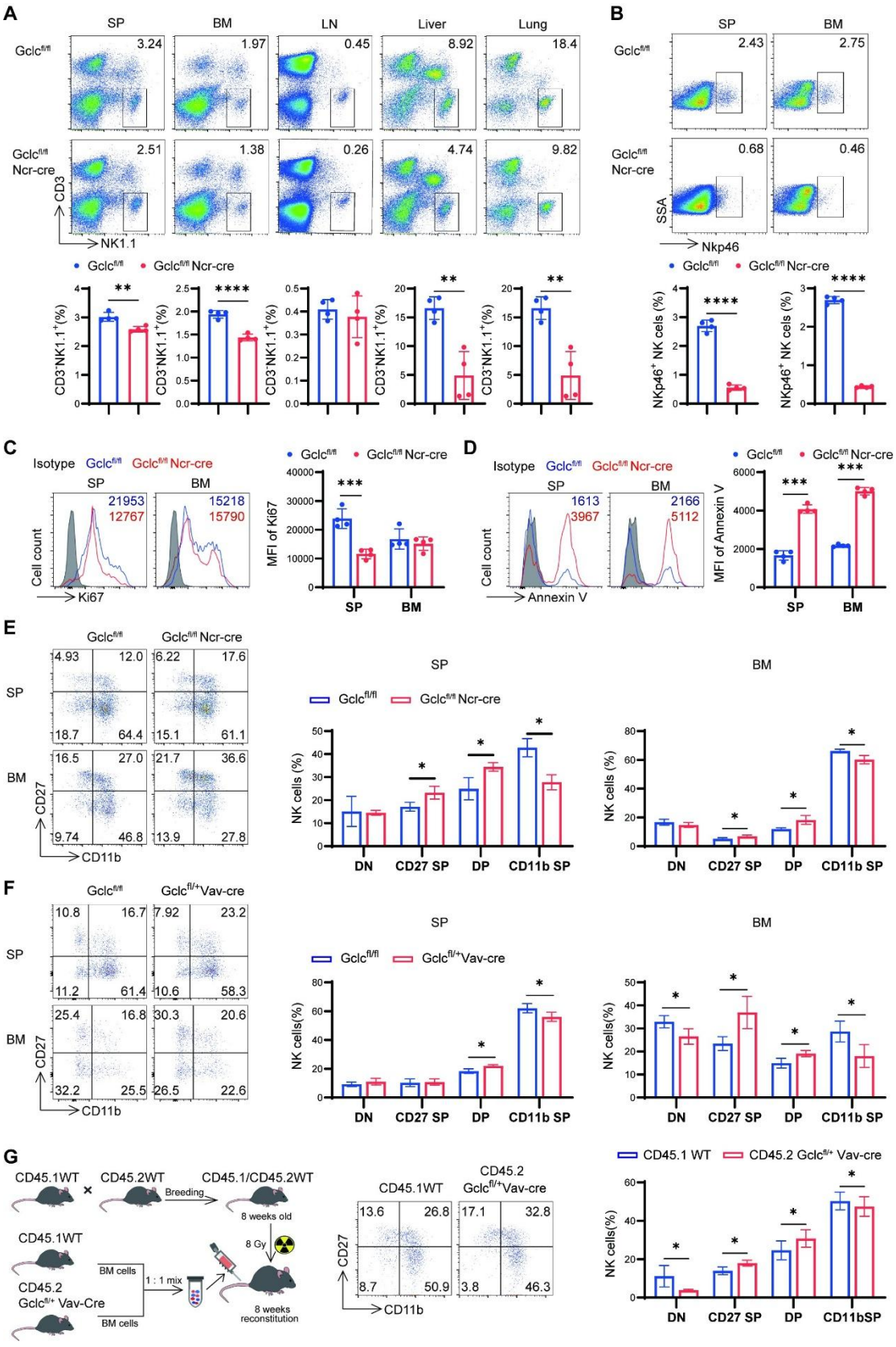
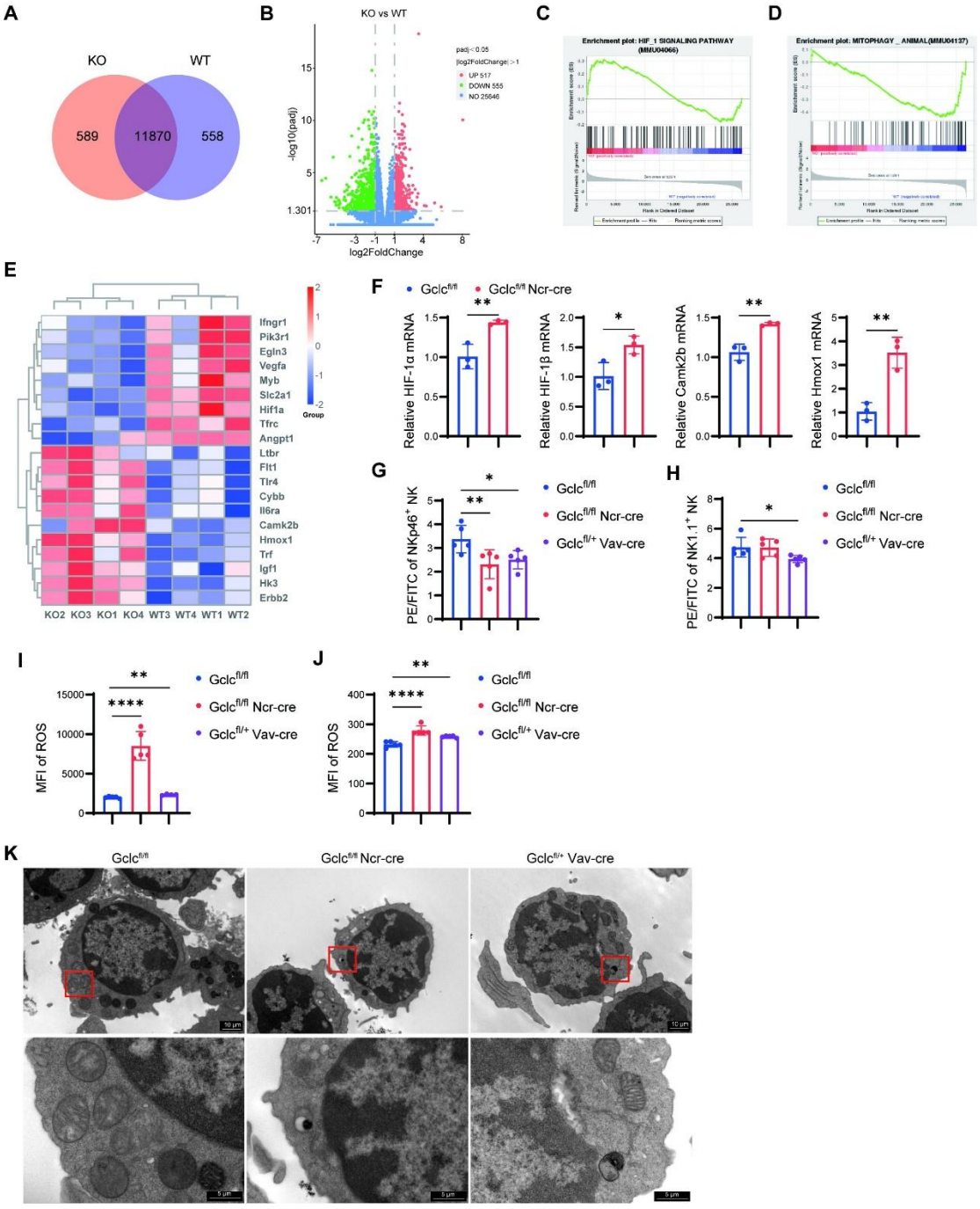

A
SP
BM
LN
Liver
Lung
Gclc fl/fl
Gclc fl/fl Ncr-cre
3.24
1.97
0.45
8.92
18.4
2.51
1.38
0.26
4.74
9.82
CD3
NK1.1
Gclc fl/fl
Gclc fl/fl Ncr-cre
CD3-NK1.1+ (%)
B
SP
BM
2.43
2.75
0.68
0.46
SSA
Nkp46
NKp46+ NK cells (%)
C
Isotype
Gclc fl/fl
Gclc fl/fl Ncr-cre
21953
12767
15218
15790
Cell count
Ki67
MFI of Ki67
SP
BM
D
1613
3967
2166
5112
Annexin V
MFI of Annexin V
E
4.93
12.0
18.7
64.4
6.22
17.6
15.1
61.1
16.5
27.0
9.74
46.8
21.7
36.6
13.9
27.8
CD27
CD11b
NK cells (%)
DN
CD27 SP
DP
CD11b SP
F
Gclc fl/+ Vav-cre
10.8
16.7
11.2
61.4
7.92
23.2
10.6
58.3
25.4
16.8
32.2
25.5
30.3
20.6
26.5
22.6
NK cells(%)
G
CD45.1WT
CD45.2WT
CD45.1/CD45.2WT
Breeding
8 weeks old
8 Gy
BM cells
1 : 1 mix
8 weeks reconstitution
CD45.2 Gclc fl/+ Vav-Cre
13.6
26.8
8.7
50.9
17.1
32.8
3.8
46.3
CD45.1 WT
CD45.2 Gclc fl/+ Vav-cre
DN
CD27 SP
DP
CD11bSP

Figure 2. GCLC supports NK-cell maintenance, survival, and terminal maturation.

A The number of $CD3^{-}NK1.1^{+}$ NK cells in the spleen, bone marrow, liver, lungs, and lymph nodes of $Gclc^{fl/fl}$ control and $Gclc^{fl/fl}$ Ncr1-cre mice. **B** $NKp46^{+}$ NK-cell numbers in $Gclc^{fl/fl}$ and $Gclc^{fl/fl}$ Ncr1-cre mice. **C** Ki67 expression in splenic and bone-marrow $NKp46^{+}$ NK cells in $Gclc^{fl/fl}$ and $Gclc^{fl/fl}$ Ncr1-cre mice. **D** Annexin V staining $NKp46^{+}$ NK cells from splenic and bone-marrow in $Gclc^{fl/fl}$ and $Gclc^{fl/fl}$ Ncr1-cre mice. **E** Distribution of NK-cell maturation subsets defined by CD27 and CD11b in the spleen and bone marrow. **F** CD27/CD11b-defined NK-cell maturation subsets in $Gclc^{fl/fl}$ and $Gclc^{fl/+}$ Vav1-cre mice. **G** Proportion of splenic NK cell subsets defined by CD11b/CD27 derived from control or $Gclc^{fl/+}$ Vav1-cre cells in competitive bone marrow chimeras, and schematic diagram of experimental design. Data are representative of, at least, 3 independent experiments and presented as means ± SEM. *P < 0.05, **P < 0.01 (n = 3 to 5).



619

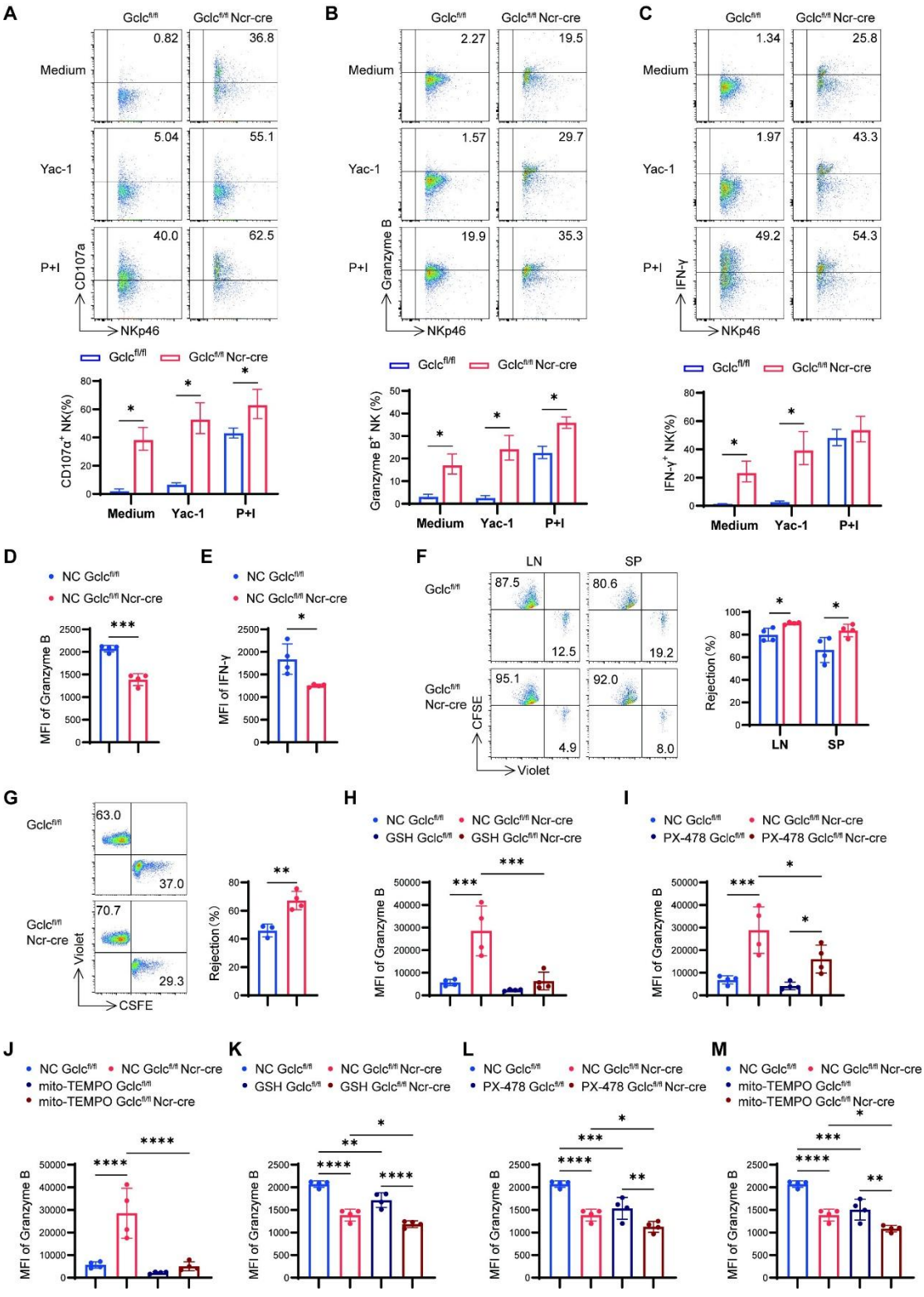
620

621 **Figure 3. GCLC deficiency is associated with altered HIF-1 signaling and mitochondrial**

622 **abnormalities in NK cells.**

623 **A** Number of genes detected in control and Gclc-deficient NK cells by RNA sequencing. **B**

Differentially expressed genes in Gclc-deficient NK cells, including 517 upregulated and 555 downregulated genes. **C, D** Gene set enrichment analysis showing enrichment of HIF-related signaling and mitophagy-associated pathways in Gclc-deficient NK cells. **E** Expression pattern of HIF-1 signaling-related genes. **F** Quantitative PCR analysis of Hif-1a, Hif-1β, Hmox1, and Camk2b transcripts in control and Gclc-deficient NK cells. **G, H** Mitochondrial membrane potential measured by JC-1 in $NKp46^{+}$ cells(G) and $CD3^{-}NK1.1^{+}$ cells(H) from the indicated mouse models. **I, J** MitoSOX fluorescence in $NKp46^{+}$ NK cells (I) and $CD3^{-}NK1.1^{+}$ NK cells(J), respectively. **K** Representative transmission electron micrographs of NK cells from $Gclc^{fl/fl}$, $Gclc^{fl/fl}$ Ncr1-cre and $Gclc^{fl/+}$ Vav1-cre mice. The lower layer image is an enlarged view of mitochondrial cristae disruption and mitochondrial autophagosomes within the red box. Data are representative of, at least, 3 independent experiments and presented as means ± SEM. *P < 0.05, **P < 0.01 (n = 3 to 5).



636

637

638 **Figure 4. GCLC deficiency uncouples NK-cell fitness from acute effector responses in a**

GSH-sensitive, HIF-1α-associated manner.

A–C Basal and YAC-1-stimulated CD107a(A), granzyme B(B), and IFN-γ(C) responses, respectively, in NKp46^{+} NK cells from Gclc$^{fl/fl}$ and Gclc$^{fl/fl}$ Ncr1-cre mice. **D, E** Granzyme B (D) and IFN-γ (E) responses in CD3^{-} NK1.1^{+} NK cells from Gclc$^{fl/fl}$ and Gclc$^{fl/fl}$ Ncr1-cre mice. **F** The relative rejection rate of β2M/WT cells injected into the tail vein by NK cells from lymph nodes and spleens of Gclc$^{fl/fl}$ and Gclc$^{fl/fl}$ Ncr1-cre mice. **G** The relative rejection rate of YAC-1/WT cells injected into the abdominal cavity by NK cells in Gclc$^{fl/fl}$ and Gclc$^{fl/fl}$ Ncr1-cre mouse peritoneal lavage fluid. **H–J** Granzyme B responses in GCLC-deficient NKp46^{+} NK cells following GSH supplementation(H), HIF-1α inhibition with PX-478(I), or mitochondrial ROS scavenging with MitoTEMPO(J), respectively. **K–M** The granzyme B response of Gclc$^{fl/fl}$ and Gclc$^{fl/fl}$ Ncr1-cre mouse CD3^{-} NK1.1^{+} NK cells after supplementation with GSH(K), PX-478(L) or MitoTEMPO(M), and the NKp46^{+} and CD3^{-} NK1.1^{+} cell populations were evaluated in parallel from the same sample under the same stimulation conditions. Data are representative of, at least, 4 independent experiments and presented as means ± SEM. Matched control-versus-treatment comparisons for GSH (H, K), PX-478 (I, L) and mito-TEMPO (J, M) were analysed using paired Student's t tests. Comparisons between two independent groups were analysed using unpaired Student's t tests. *$P < 0.05$, **$P < 0.01$ ($n = 4$).

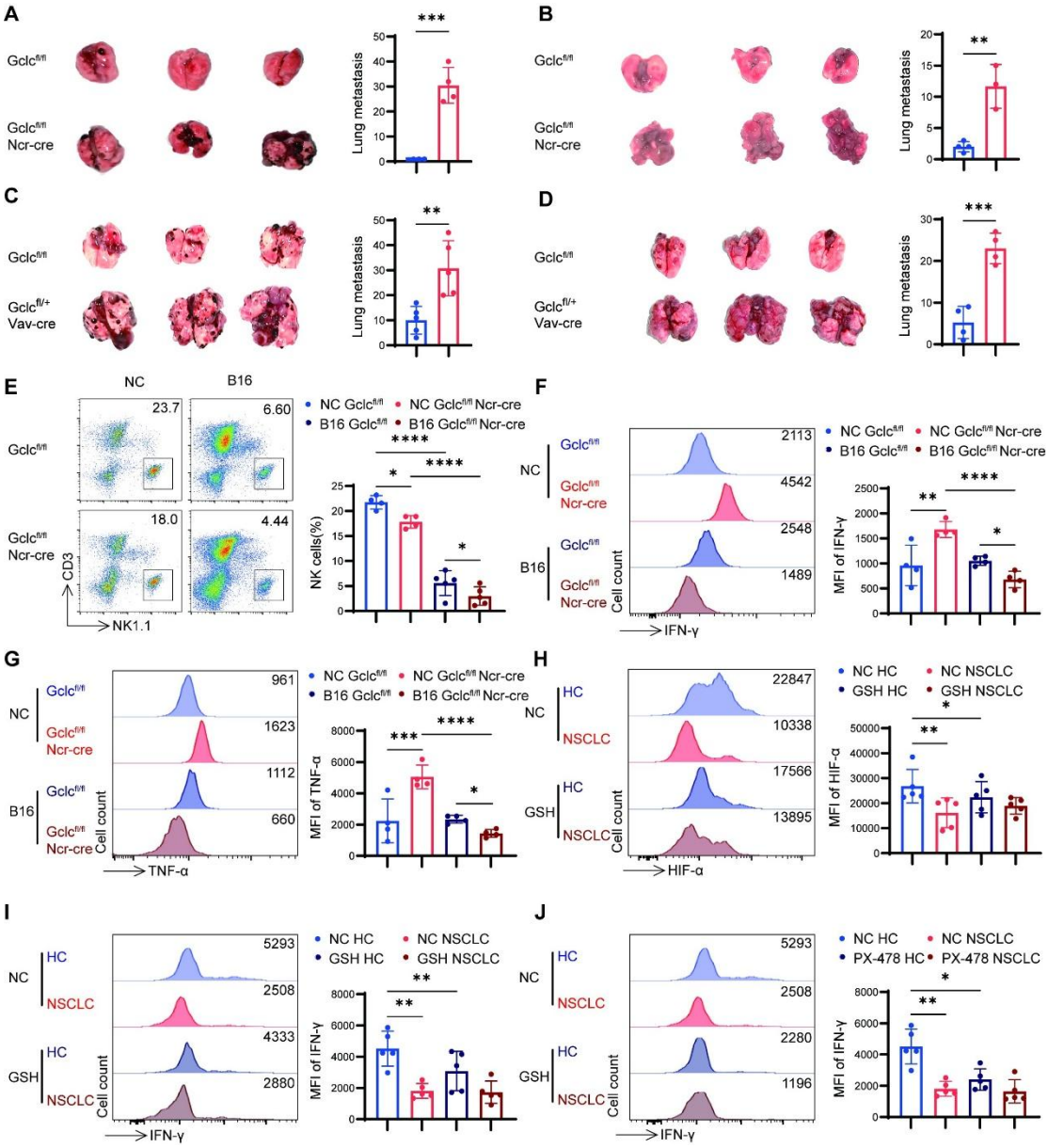


Figure 5. GCLC deficiency impairs NK-cell abundance, function, and tumor control in tumor-bearing mice.

A Lung tumor burden in Gclc$^{fl/fl}$ and Gclc$^{fl/fl}$ Ncr1-cre mice in the B16 pulmonary metastasis model. **B** Tumor growth in the LLC model. **C** B16 metastatic burden in Gclc$^{fl/fl}$ and Gclc$^{fl/+}$ Vav1-cre mice. **D** LLC tumor growth in Gclc$^{fl/fl}$ and Gclc$^{fl/+}$ Vav1-cre mice. **E** The proportion

of NK cells in lung tissue of normal mice and B16 tumor bearing mice. **F, G** Expression of IFN-γ (F) and TNF-α (G) on NK cells in lung tissues of normal mice and B16 tumor bearing mice. **H** The mean fluorescence intensity of HIF-1α in NK cells by healthy donors and NSCLC patients after supplementing GSH. **I, J** The mean fluorescence intensity of IFN-γ in NK cells by healthy donors and NSCLC patients after supplementing GSH (I) or inhibiting HIF-1α with PX-478 (J). Data are representative of, at least, 3 independent experiments and presented as means ± SEM. Matched control-versus-treatment comparisons for GSH (H, I) and PX-478 (J) were analysed using paired Student's t tests. Comparisons between two independent groups were analysed using unpaired Student's t tests. *P < 0.05, **P < 0.01 (n = 3 to 5).

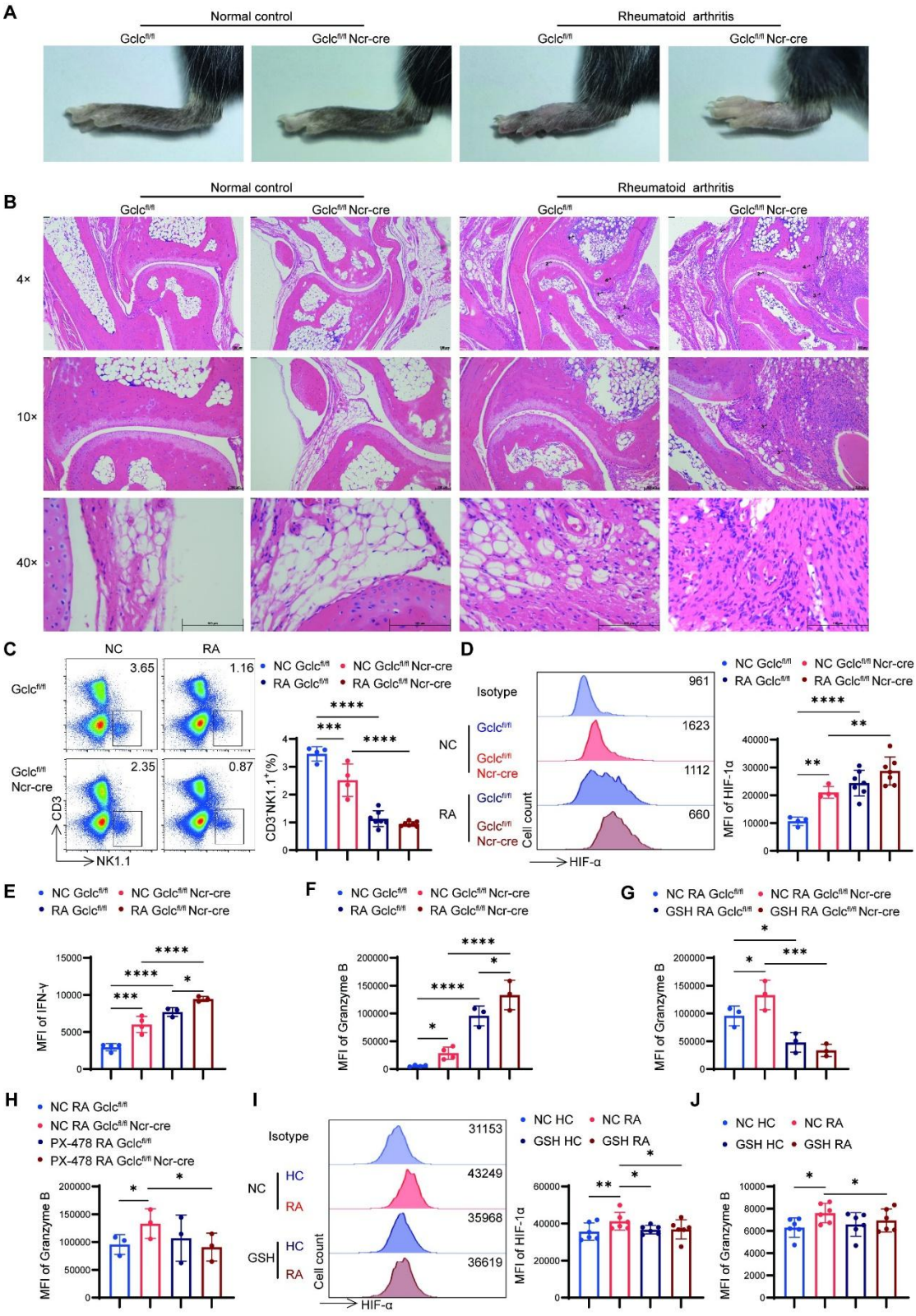
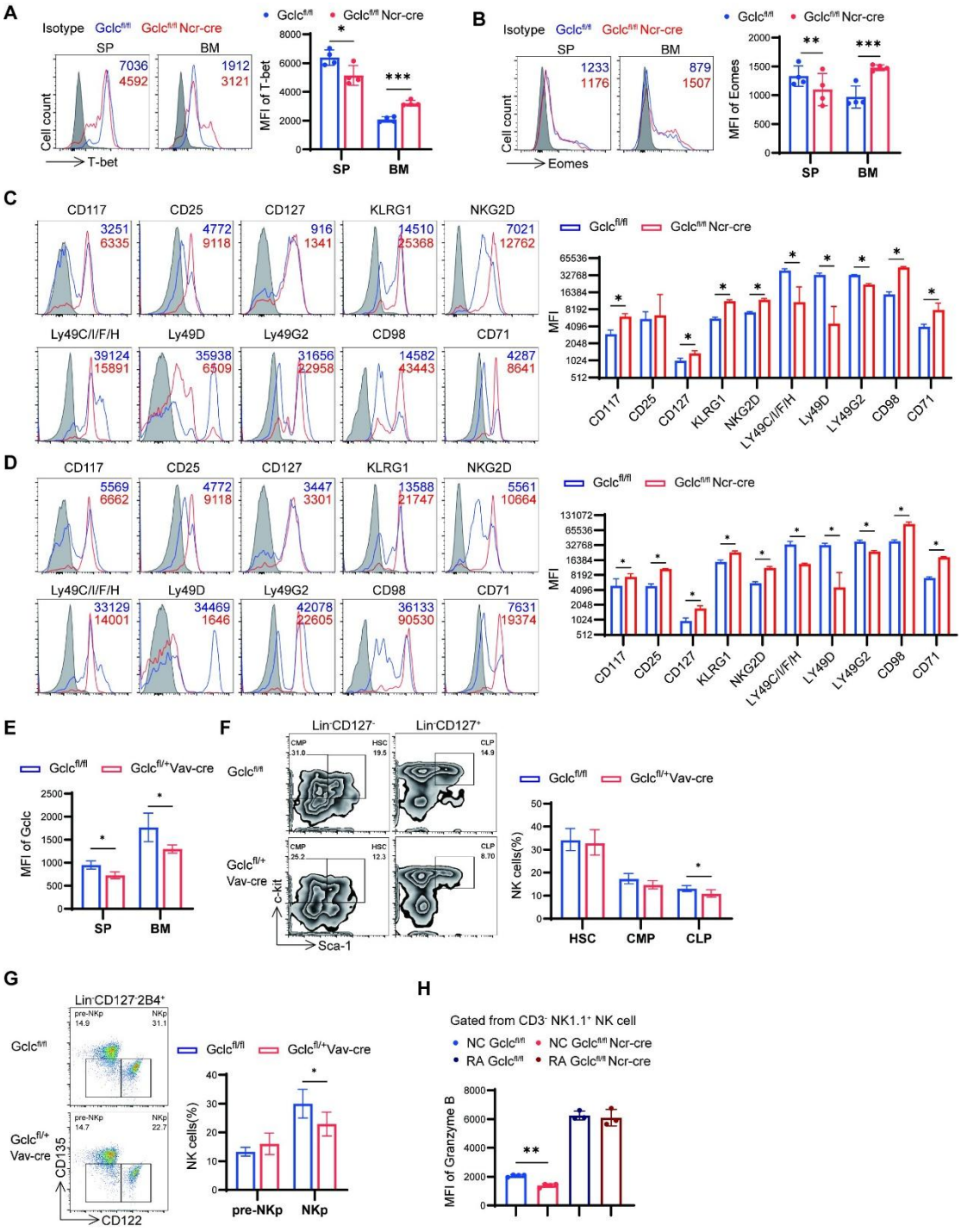


Figure 6. GSH supplementation and HIF-1α inhibition reduce elevated NK-cell

granzyme B responses in inflammatory arthritis.

A Representative gross appearance of ankle joints from control and rheumatoid arthritis mice with or without Ncr1-cre-mediated Gclc deletion. **B** Representative ankle-joint histology showing synovial hyperplasia(40×), inflammatory-cell infiltration(1), inflammatory cell exudation in the joint cavity(2), pannus-like tissue(3) and cartilage abnormalities(4). **C,D** Splenic NK-cell proportion (C), HIF-1α expression in NK cells (D) from healthy control and RA model mice carrying $Gclc^{fl/fl}$ and $Gclc^{fl/fl}$ Ncr1-cre mice. **E,F** MFI of IFN-γ (E) and granzyme B (F) in NK cells from healthy control and RA model mice carrying $Gclc^{fl/fl}$ and $Gclc^{fl/fl}$ Ncr1-cre mice. **G, H** Granzyme B responses in splenic NK cells from healthy control and RA model mice carrying the indicated genotypes after GSH supplementation (G) or HIF-1α inhibition (H). **I, J** HIF-1α expression (I) and granzyme B expression (J) in NK cells from healthy donors and RA patients after GSH supplementation. Data are representative of, at least, 3 independent experiments and presented as means ± SEM. Comparisons between two independent groups were analysed using unpaired Student's t tests. *$P < 0.05$, **$P < 0.01$ ($n = 3$ to 6).



Supplementary Figure 1. GCLC deficiency alters NK-cell transcription-factor expression, progenitor abundance, and maturation-associated markers.

(A) T-bet expression in NK cells from the spleen and bone marrow of $Gclc^{fl/fl}$ and $Gclc^{fl/fl}$ Ncr1-cre mice. (B) Eomes expression in NK cells from the spleen and bone marrow of $Gclc^{fl/fl}$ and $Gclc^{fl/fl}$ Ncr1-cre mice. (C) The expression of cell surface receptors such as CD117, CD127, and Ly49 family receptors in splenic NK cells after Gclc deficiency. (D) The expression of cell surface receptors such as CD117, CD127, and Ly49 family receptors in bone marrow NK cells after Gclc deficiency. (E) GCLC expression in the in $Gclc^{fl/fl}$ and $Gclc^{fl/+}$ Vav1-cre mice. (F) Abundance of hematopoietic stem cells (HSC), common myeloid progenitors(CMP), common lymphoid progenitors(CLP) in $Gclc^{fl/fl}$ and $Gclc^{fl/+}$ Vav1-cre mice. (G) Abundance of pre-NK progenitors(pre-NKp), and NK progenitors(NKp) in $Gclc^{fl/fl}$ and $Gclc^{fl/+}$ Vav1-cre mice. (H) Granzyme B expression in $CD3^{-}$ $NK1.1^{+}$ NK cells from healthy control and RA model mice carrying $Gclc^{fl/fl}$ and $Gclc^{fl/fl}$ Ncr1-cre mice. Data are representative of, at least, 3 independent experiments and presented as means ± SEM. *P < 0.05, **P < 0.01 (n = 3 to 5).